CCFE
CULHAM CENTRE FOR FUSION ENERGY

UK Atomic Energy Authority

UKAEA-CCFE-CP(19)41

S.N. Gerasimov, G Artaserse, P. Buratti, I.S. Carvalho, E. de la Luna, T.C. Hender, R.B. Henriques, P.J. Lomas, E. Matveeva, S. Moradi, L. Piron, F.G. Rimini, G. Szepesi, L.E. Zakharov, JET Contributors

Locked mode and disruption in JET-ILW

Locked mode and disruption in JET-ILW

S.N. Gerasimov, G Artaserse, P. Buratti, I.S. Carvalho, E. de la Luna, T.C. Hender, R.B. Henriques, P.J. Lomas, E. Matveeva, S. Moradi, L. Piron, F.G. Rimini, G. Szepesi, L.E. Zakharov, JET Contributors

This paper has been submitted to
46th European Physical Society Conference on Plasma Physics (EPS), Milan, 8-12 July 2019

Locked mode and disruption in JET-ILW

S.N. Gerasimov[1], P. Abreu[2], G. Artaserse[3], P. Buratti[3], I.S. Carvalho[2], E. de la Luna[4], E. Giovannozzi[3], T.C. Hender[1], R.B. Henriques[2], P.J. Lomas[1], E. Matveeva[5,6], S. Moradi[7], L. Piron[8], F.G. Rimini[1], H. Sun[1], G. Szepesi[1], L.E. Zakharov[9,10,11] and JET Contributors[*]

EUROfusion Consortium, JET, Culham Science Centre, Abingdon, OX14 3DB, UK

[1] *UKAEA/CCFE, Culham Science Centre, Abingdon, Oxon, OX14 3DB, UK*
[2] *Instituto de Plasmas e Fusão Nuclear, Instituto Superior Técnico, Universidade de Lisboa, Portugal*
[3] *ENEA for EUROfusion, via E. Fermi 45, 00044 Frascati (Roma), Italy*
[4] *Laboratorio Nacional de Fusión, CIEMAT, 28040 Madrid, Spain*
[5] *Charles University, Faculty of Mathematics and Physics, Prague, Czech Republic*
[6] *Institute of Plasma Physics of the CAS, Prague, Czech Republic*
[7] *Laboratory for Plasma Physics - LPP-ERM/KMS, Royal Military Academy, 1000-Brussels, Belgium*
[8] *Università di Padova and Consorzio RFX, Corso Stati Uniti 4, 35127, Padova, Italy*
[9] *LiWFusion P.O. Box 2391, Princeton NJ 08543, USA*
[10] *Department of Physics, University of Helsinki, P.O. Box 43, FIN - 00014, Finland*
[11] *Department of Plasma Physics, National Research Nuclear University MEPhI, 115409, Moscow, RF*

An n = 1 locked, or slowly rotating, mode has been observed in most pulses prior to JET disruptions [1]–[4]. However, a small fraction of non-disruptive pulses has a locked mode (LM) which eventually vanishes without disruption. Despite these exceptions the LM Saddle (LMS) amplitude is routinely used as a trigger for the JET disruption avoidance and protection systems. There are two threshold levels of the LM amplitude: (i) if the LMS amplitude exceeds the "low" threshold level, the fast pulse shutdown is activated; (ii) if the LMS amplitude exceeds the "high" threshold level, the Massive Gas Injection (MGI) is triggered to terminate the pulse because the plasma is at high risk of disruption, and so it is necessary to mitigate disruption damage to the vessel and the Plasma Facing Components (PFC). The n = 1 LM amplitude and phase can be

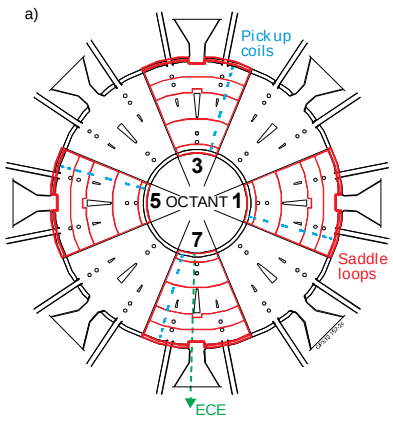

Fig. 1 JET magnetic diagnostics and ECE locations (a) Plan view, (b) Vessel octant.

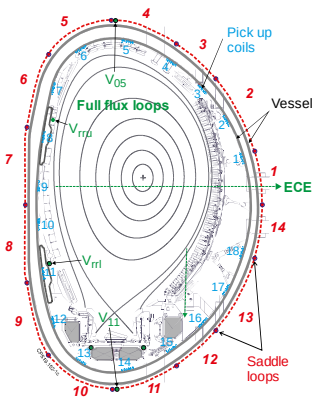

Fig. 2 JET vessel poloidal cross-section.

calculated either from a subset of the four saddle loops (LMS signal) or the four pick-up coils (LMC signal) located at identical poloidal locations, Fig. 1 and Fig. 2. The saddle loops measure the normal to the vessel component of the poloidal magnetic field (B_n) and the pick-up coils measure the tangential component of the field (B_τ). The ECE (Electron Cyclotron Emission) line of sight is

[*] *See the author list of "Overview of the JET preparation for Deuterium-Tritium Operation" by E. Joffrin et al. to be published in Nuclear Fusion Special issue: overview and summary reports from the 27th Fusion Energy Conference (Ahmedabad, India, 22-27 October 2018)*

located near the center of octant 7, just above the middle plane of the vessel which usually corresponds approximate height of the magnetic axis.

During 2011-2016 JET-ILW operation, 1951 disruption pulses occurred [5]. For the presented LM analysis, a subset of 912 "natural" disruptions has been used: without VDE (Vertical Displacement Event), EFCC (Error Field Correction Coils) and MGI, but with late (after disruption) MGI pulses. It is worth mentioning that the majority (more than 93%) of the 912 "natural" disruptions happened during plasma termination phase, either planned or triggered by off-normal events. The locked mode amplitude *LocaN* is calculated from saddles 1+14 (Fig. 1) with parasitic offset removed and normalised by plasma current (I_p). The *LocaN* waveforms significantly vary prior to a disruption from pulse to pulse, Fig. 3. The low-density plasmas, with line-averaged normalised density $\leq 1 \cdot 10^{19}$ $m^{-3}MA^{-1}$, manifest a smooth long continuous increase of the *LocaN* prior to (minor or major) disruptions (see blue trace on Fig. 3). However, in the majority of the pulses *LocaN* signal has a complicated behaviour (see red and magenta traces on Fig. 3). Moreover, in some pulses *LocaN* signal has a low amplitude prior to a disruption (see green trace on Fig. 3). It is worth mentioning that minor disruptions always trigger a LM signal, which will remain until of the end of a pulse.

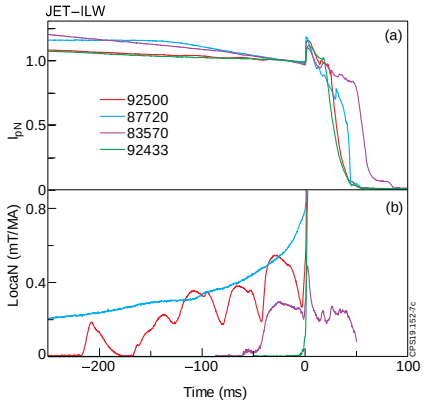

Fig. 3 Examples of various normalised LM saddle waveforms -(b), I_p normalised by pre-disruptive plasma currents -(a). The time axis is zeroed to Tdis.

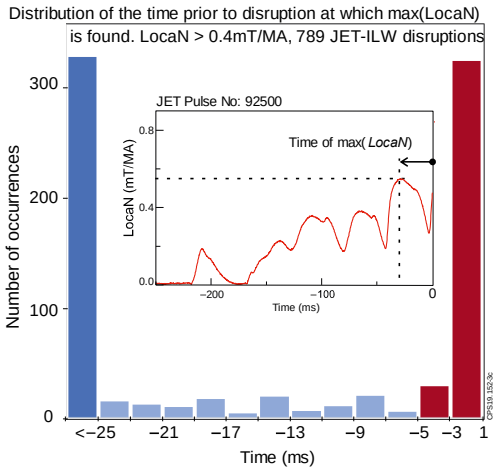

Fig. 4 Distribution of max(LocaN) time prior to disruption. Inset illustrates max(LocaN) time calculation.

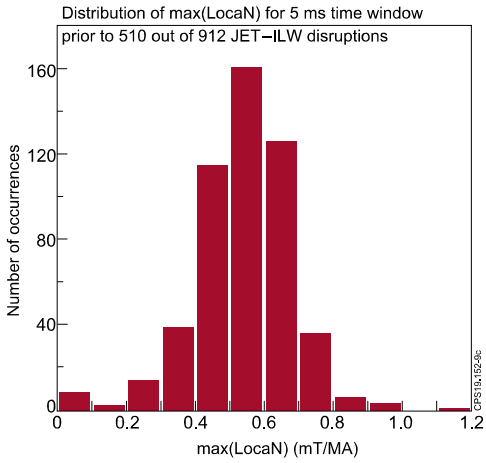

Fig. 5 Distribution of max(LocaN) prior to disruption.

The *LocaN* exceeds the 0.4 mT/MA (which was a standard threshold to trigger MGI) for 789 out of 912 pulses. For this subset of 789 pulses, the distribution of the time prior to disruption, at which the maximum value of *LocaN* is found, is shown in Fig. 4. The *LocaN* has a maximum value just before disruption only in ~50% of the pulses. In the other half of the pulses, *LocaN* has

a maximum value significantly earlier than the disruption. This suggests that a locked mode is not always directly responsible for disruptions. Moreover, Fig. 5 shows the distribution of maximum *LocaN* for all pulses in which *max(LocaN)* is found in the 5 ms time window prior to disruption. It can be seen that there is no obvious magnitude of the LocaN which correlated with disruption triggering. Thus, even for pulses where *LocaN* has a maximum value just before disruption (Fig. 5), it can be concluded that the locked mode saddle signal should not be used as a disruption predictor. However, we believe there is an exception when the LMS signal is a good predictor of minor or major disruptions: it is low density plasmas which are associated with growing error field locked mode, see blue trace on Fig. 3. These low-density pulses are related to various human or technical density control faults. It is highly likely, that for these pulses, the locked mode was a primary reason for disruptions. Fig. 6 displays the distribution of time prior to disruption at which *LocaN* reaches a specified threshold. In the majority of the pulses (87%) *LocaN* reaches a value of 0.4 mT/MA, but this occurs usually in hundreds of milliseconds prior to disruption. A value of 0.6 mT/MA reaches in 34% of the pulse but again in many cases this happens significantly before the disruption occurred. A value of 0.8 mT/MA is reached in a small fraction of pulses, 3%. In the majority of the pulses (96%) *LocaN* was above the value of 0.2 mT/MA, at which the fast pulse shutdown is generally activated.

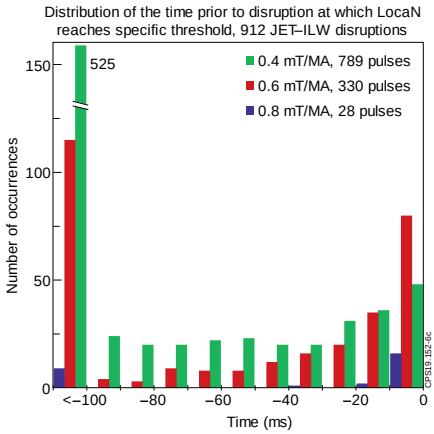

Fig. 6 Distribution of the time prior to disruption at which LocaN reaches a specific threshold.

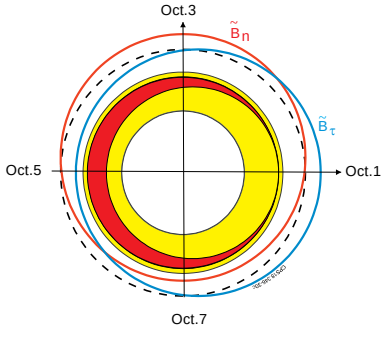

Fig. 7 Illustration of magnetic field components for n=1 island (in red), plan view.

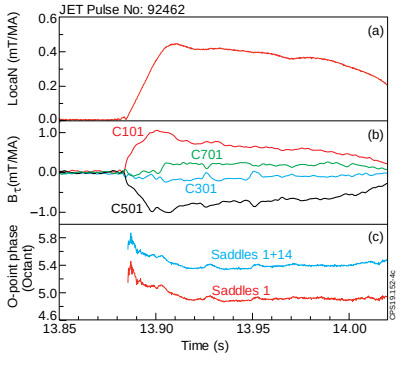

Fig. 8 Coil data (B_τ) used for saddle (B_n) phase calibration.

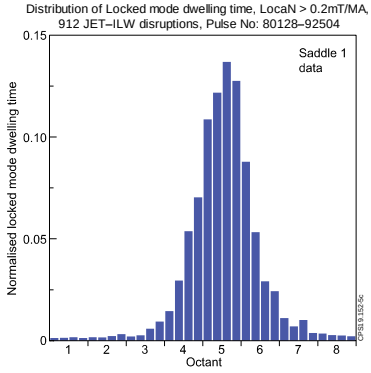

Fig. 9 Distribution of the normalised locked mode time, Saddle 1 data.

It is better to calculate the locked mode toroidal phase from saddle 1 than saddle 1+14 data, taking into account the location of the magnetic sensors (see Fig. 2). For monotonic plasma current profile, the O-point of the tearing mode island corresponds to a reduction of the B_τ. Fig. 7

illustrates the island location for pulse #92462 with $q_{95} = 4.0$, where B_τ (absolute value) reduces at octant 5 and increases at octant 1, as can be seen in Fig. 8. Using this observation, the phase of LMS is calibrated. The difference of ~ π/8 in Saddle 1 and Saddle 1+14 phase reflects the effect of helicity on phase data. The O-point of the locked mode has a preferred toroidal phase dwelling mainly in octant 5, as a consequence of the machine toroidal asymmetries, Fig. 9. The distribution is the result of the composition of many pulses with different phase behavior.

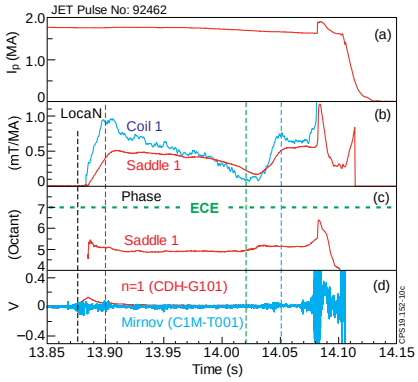

Fig. 10 Typical pulse where locked mode precedes the disruption.

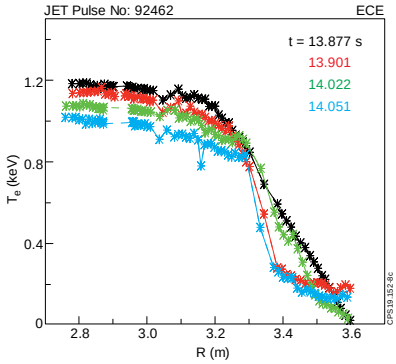

Fig. 11 Te profiles during LM evolution shown in Fig. 10.

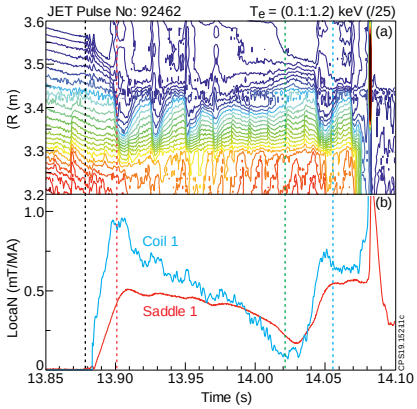

Fig. 12 (a) Te contour, ECE data; (b) LM amplitudes.

ECE data, when it is valid, can be compared with magnetic data. Fig. 10 shows the typical pulse in which a LM precedes the disruption. The T_e profiles for four specific times and T_e contours are illustrated in Fig. 11 and Fig. 12. The LM coils respond faster than the LM saddles and the variation in amplitude is larger, which was expected because the saddle B_n is screened by the vessel and does not correctly reflect the instantaneous LM amplitude. There is a general consistency between magnetics and ECE data: the time slices with large values of *LocaN* correspond to T_e flattening in R ~ [3.3:3.6] m region. However, the fine T_e contour structure, which can be seen during t = [13.90:13.97] s on Fig. 12, is not clearly visible either by saddles or by coils.

Summary: These studies reveal that for the majority of JET pulses the Locked Mode Saddle (LMS) signal is not a good predictor of disruptions, but the LMS usually precedes disruptions. For JET, the 0.8 mT/MA threshold could be used for MGI triggering for the low-density LM disruption. Low LM threshold (0.2 mT/MA) may be used for JET pulse fast shutdown because it is a good indicator of unhealthy plasma conditions.

This work has been carried out within the framework of the EUROfusion Consortium and has received funding from the Euratom research and training programme 2014-2018 and 2019-2020 under grant agreement No 633053 and from the RCUK Energy Programme [EP/P012450/1]. To obtain further information on the data and models underlying this paper please contact PublicationsManager@ukaea.uk. The views and opinions expressed herein do not necessarily reflect those of the European Commission.

[1] J. A. Snipes *et al.*, "Large amplitude quasi-stationary MHD modes in JET," *Nucl. Fusion*, **28**, p.1085, 1988.
[2] J. A. Wesson *et al.*, "Disruptions in JET," *Nucl. Fusion*, **29**, p.641, 1989.
[3] J. A. W. M.F.F. Nave, "Mode locking in tokamaks," *Nucl. Fusion*, **30**, p.2575, 1990.
[4] P. C. De Vries *et al.*, "The influence of an ITER-like wall on disruptions at JET," *Phys. Plasmas*, **21**, 2014.
[5] S. N. Gerasimov *et al.*, "Overview of disruptions with JET-ILW," *Proc 27th IAEA Fusion Energy Conf. (Ahmedabad, India) EX/P1-24*, 2018.